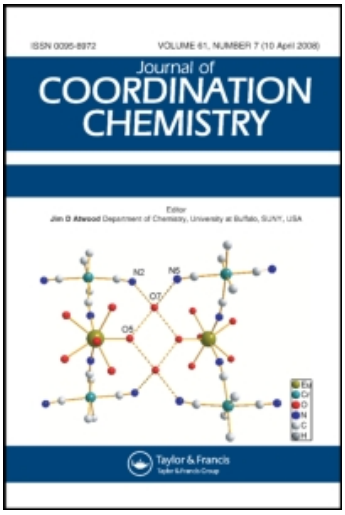

Journal of Coordination Chemistry
Publication details, including instructions for authors and subscription information:
http://www.informaworld.com/smpp/title~content=t713455674

Study on the properties of the photoluminescence material Tb(aspirin)$_3$phen-MCM-41

Bin Zhou[ab]; Chang Ping Wei[a]; Chun Jia Peng[a]; Yue Chun Yu[b]
[a] College of Materials Science and Engineering, Changchun University of Science and Technology, Changchun 130022, China [b] College of Optical and Electronical Information, Changchun University of Science and Technology, Changchun 130012, China

First published on: 11 June 2010

To cite this Article Zhou, Bin , Wei, Chang Ping , Peng, Chun Jia and Yu, Yue Chun(2010) 'Study on the properties of the photoluminescence material Tb(aspirin)$_3$phen-MCM-41', Journal of Coordination Chemistry, 63: 10, 1752 — 1762, First published on: 11 June 2010 (iFirst)
To link to this Article: DOI: 10.1080/00958972.2010.490581
URL: http://dx.doi.org/10.1080/00958972.2010.490581

Journal of Coordination Chemistry
Vol. 63, No. 10, 20 May 2010, 1752–1762

Taylor & Francis
Taylor & Francis Group

Study on the properties of the photoluminescence material Tb(aspirin)$_3$phen-MCM-41

BIN ZHOU†‡, CHANG PING WEI*†, CHUN JIA PENG†
and YUE CHUN YU‡

†College of Materials Science and Engineering, Changchun University of Science and Technology, Changchun 130022, China
‡College of Optical and Electronical Information, Changchun University of Science and Technology, Changchun 130012, China

(*Received 24 June 2009; in final form 2 March 2010*)

Assembly system with MCM-41 as a host and TAP (Tb(aspirin)$_3$phen) as an active optical guest was synthesized at room temperature, and the interrelated products of MCM-41 and TAP systems were examined for comparison. The structures and the physical properties of the samples were characterized by a combination of techniques, such as XRD and N_2 adsorption–desorption. Excitation and emission spectra were carried out to explore the photoluminescence (PL) properties of the samples and the relationships between the optical guest and the inorganic host. The results from these characterizations showed that the TAP is incorporated into the channels of MCM-41 and can increase the framework order of MCM-41. The reduction in the specific surface area of TAPMA (Tb(aspirin)$_3$phen-MCM-41A) compared with that of MA (MCM-41A) imply that the TAP is confined inside the channels of MA. Based on the analyses of the excitation spectra, we suggested that the surface environment of MCM-41 affects the energy absorption of the organic ligands. PL of TAPMA and TAPMB show TAP in the different chemical environments, and a strong green PL had been observed in the TAPMA system while a much weaker light in the TAPMB system.

Keywords: Tb(aspirin)$_3$phen-MCM-41; Assembly; Properties; Photoluminescence

1. Introduction

Mesoporous materials, M41S, were discovered in 1992 by researchers at Mobil Oil Corporation [1]. MCM-41 attracts strong attention of many scientists for its interesting features, such as a 1-D, hexagonally ordered pore structure, adjustable pore size (1.5–20 nm), high pore volumes ($>0.6\,cm^3\,g^{-1}$), high specific surface area up to $1000\,m^2\,g^{-1}$, large quantity of internal silanol groups (40–60%) [2] and high thermal, chemical, and mechanical stability [3]. Ordered MCM-41 materials have been widely studied for application in fields, such as catalysis [4–6] and drug release [7, 8]. In addition, MCM-41 is promising host material for optical functionalities which may have potential applications in optoelectronics recording [9–11], because of its chemical micro-environment provided by the nano-diameter channels.

*Corresponding author. Email: changpingwei@yahoo.com.cn

ISSN 0095-8972 print/ISSN 1029-0389 online © 2010 Taylor & Francis
DOI: 10.1080/00958972.2010.490581

Photoluminescence (PL) properties of a rare earth complex within MCM-41 are new and important characteristics both from optical physics and assembly chemistry point of view. Not only the nature of PL of the organic or inorganic compound, but also the interaction between the organic and inorganic compounds can be elucidated from the study on the PL properties of MCM-41 assembly systems, providing useful information for extending their applications to optical devices.

Common solutions to increase the interaction efficiency between the host and the guest are to modify the surface of MCM-41 to enhance its polarity by chemical methods [12, 13]. Based on our research, those methods also will decrease the framework order, the specific surface area, and the pore diameter of MCM-41 to a certain degree, which are the disadvantages for its practical applications. These chemical modifications also cannot enhance the PL properties of rare earth ions efficiently, even inducing ions into a lower level compared with the pure rare earth complex powder.

This article introduces a new synthesis process for TAP to avoid the adverse influence on framework order of MCM-41 by using heat treatment process. In this work, we investigate the structure of the assembly systems and discuss relationships between host and guest by a combination of different techniques. Some suitable explanations are introduced to describe the special PL regularity in the different composite systems, such as the effects of the different silica surfaces on the energy absorption of organic ligands. A simple method to present the PL phenomenon is introduced, the PL photos of TAPMA and TAPMB, which is the most visual proof for existence of TAP in the pores of MCM-41.

2. Experimental

2.1. *Sample preparations*

As many products have been synthesized in this work, abbreviations are shown in table 1. M was prepared from EDA (ethylenediamine) solution at room temperature using the following molar ratios: 1 TEOS (tetraethyl orthosilicate)/0.1 CTAB (cetyltrimethylammonium bromide)/0.25 EDA/100 H_2O. The product was filtered and washed to neutral pH, and then MB (MCM-41B, MCM-41 before the template-removing process, called calcination) was obtained. MA (MCM-41A, after the

Table 1. Abbreviations for the solid products.

Abbreviation	Products
M	MCM-41
MA	MCM-41A
MB	MCM-41B
TAP	$Tb(aspirin)_3phen$
TAPM	$Tb(aspirin)_3phen$-MCM-41
TAPMA	$Tb(aspirin)_3phen$-MCM-41A
TAPMA-b	$Tb(aspirin)_3phen$-MCM-41A-b
TAPMB	$Tb(aspirin)_3phen$-MCM-41B
TAPMB-b	$Tb(aspirin)_3phen$-MCM-41B-b

template-removing process) was further obtained by calcination at 550°C for 3 h, removing the template CTAB.

Although the synthesis of TAP ($Tb(aspirin)_3phen$, where the phen is the 1,10-phenanthroline) had been reported [14, 15], in this article we introduced a new synthesis, heat treating, for TAP, which is more suitable for MA. The original complex solution was heated for crystallization, then filtered and washed product to neutral pH, and dried under vacuum, giving TAP.

Assembly system TAPM was synthesized by the self-assembly reaction between MA (or MB) and TAP in solution. In this procedure, 0.1 g TAP, 20 mL ethanol, 2 mL DMF, and 0.5 g MA (or MB) were stirred for 2 h, filtered, washed to neutral pH, dried at 100°C under vacuum, and then TAPMA (or TAPMB) was obtained.

Physical mixture TAPMA-b (or TAPMB-b) of TAP and MA (or MB) was also obtained by grinding for 30 min.

All the samples were protected by nitrogen before characterized.

2.2. *Characterizations*

X-ray powder diffraction patterns were recorded by a Japan Rigaku D/max-rA X-ray diffractometer equipped with graphite monochromated Cu-Kα radiation ($\lambda = 0.154178$ nm) at a scanning rate of 0.02°/s in 2θ ranging from 1.5° to 10°, 50 KV (tube voltages), 150 mA (tube current). The specific surface area, average pore diameter, and total pore volume were obtained from N_2 adsorption/desorption at −196°C using a Quanta Chrome NOVA 1000 instrument and the samples were activated at 180°C for 6 h under vacuum. The specific surface area was estimated by application of BET equation, total pore volume from the N_2 adsorbed at $P/P_0 \leq 0.95$, and the pore size distribution obtained by applying the BHJ pore analysis method. Nicolet 1TOSX equipment was used to obtain FT-IR spectra of the prepared samples over a measuring range of 400–4000 cm^{-1} using KBr pellets. TG-DTA was carried out in 100 mL min^{-1} air using a TA Instruments, SDT2960 from 25°C to 851°C at a heating rate of 10°C min^{-1}. The fluorescence excitation and emission spectra were performed on a HITACHI F-4500 FL spectrophotometer at 700 V (PMT voltage) at room temperature at 1200 nm min^{-1}.

3. Results and discussion

3.1. *X-ray diffraction*

XRD diffraction patterns of MA (MCM-41A, MCM-41 after the template-removing process) and TAPMA ($Tb(aspirin)_3phen$-MCM-41A, the assembly system of TAP and MA) are provided in figure 1. A strong reflection at $2\theta = 2.62$ attributed to (100) reflection present in both XRD patterns of the two samples is always observed for regular, spherical structure of MCM-41. Two peaks between 4 and 6 attributed to (110) and (200) reflections appear in the patterns. The patterns show that both MA and TAPMA are typical hexagonally ordered MCM-41 materials. The main difference between the two XRD patterns is the relative intensity of the peak at $2\theta = 2.62$, which increases after assembly. We suggest that the TAP incorporated into the channels

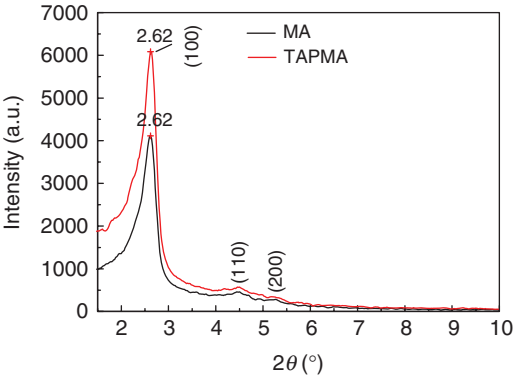

Figure 1. XRD patterns of TAPMA and MA.

Table 2. Physical parameters of MA and TAPMA.

Parameter	MA	TAPMA
θ°	2.62	2.62
d_{100}[a] (nm)	3.3692	3.3692
a_0[b] (nm)	3.8905	3.8905
D[c] (nm)	2.9020	3.1621
T[d] (nm)	0.9885	0.6989
S_{BET} (m)^2 g^{-1}	1378.4077	912.4172
V[e] (cm)^3 g^{-1}	1.00003	0.73271

[a]$d = \lambda/2\sin\theta$.
[b]Unit cell dimension $a_0 = 2d_{100}/\sqrt{3}$ [16].
[c]Average pore diameter according to BJH method.
[d]Thickness of pore wall, $T = a_0 - D$.
[e]Volume, BET transform: $1/W(P_0/P - 1)$.

enhances the lattice order of the siliceous surface of MCM-41A. The data of d_{100}, a_0, and other physical parameters are presented in table 2, from which it can be seen that TAP has no effect on the cell parameters or unit structure because no shift of the first peak occurs.

3.2. *N_2 Adsorption/desorption*

N_2 adsorption–desorption isotherms of MA and TAPMA at −196°C are shown in figure 2. Both of the isotherms are of type IV classification with an inflection at $P/P_0 = 0.2$–0.3 attributed to the capillary condensation of N_2 molecules, and are typical adsorption mesoporous materials having uniform mesoporous structure with high order according to IUPAC nomenclature [17]. The values of pore volume V and average pore diameter D are calculated by using BET equation, and the thickness (T) of the pore wall is calculated as $T = a_0 - D$ from the cell parameter a_0 and the pore diameter D. All the values are given in table 2. Compared with MA, the specific surface area S_{BET} of TAPMA decreases by 465.9905 m^2 g^{-1}, D increases by 0.2601 nm, and T decreases by 0.2601 nm, indicating that TAP has been confined inside the channels of MA.

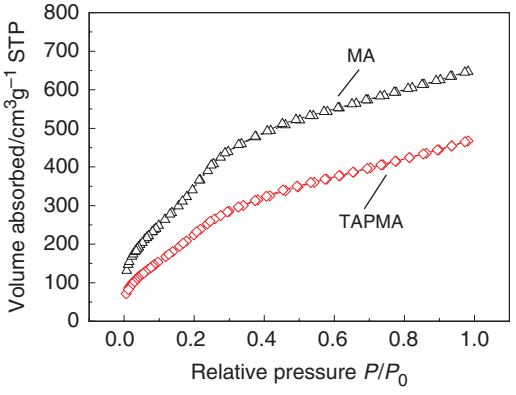

Figure 2. N_2 adsorption–desorption isotherms of MA and TAPMA at −196°C.

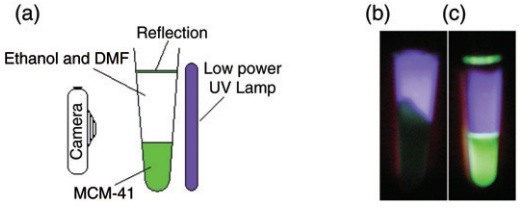

Figure 3. (a) Units of photo taking system for PL property using a low power UV-lamp (4 W) in a dark box; (b) photo of TAPMB; (c) photo of TAPMA.

3.3. *Photoluminescence*

PL photos of the centrifuged TAPMB and TAPMA in mixture of ethanol and DMF solution at the bottom of the centrifugal tubes were taken in a dark box by using a low power UV-lamp (1 W), and the photographs are shown in figure 3. A schematic view of the two systems is shown in figure 4. Obviously, TAPMA has strong green PL even under the low power UV-lamp, while only very weak green light is emitted from TAPMB. This can be explained by two aspects, first, MA absorbs a higher content of TAP on its surface, including the internal and the external surfaces, than the MB system; and second, TAP has readily been embedded into channels of MA. According to the results from the FI-IR spectra, it is impossible for all TAP absorbed by MA to emit such a high intensity of green light if absorbed just on the external surface in an extremely low content. Figure 3(b) also implies that only a few TAP can make bonds with the silanol groups on the external surface to emit weak light, and the most distributed in the mixture solution cannot be excited by UV light. We suggest that the origin of green light emission depends on the separating TAP from the surrounding solvent molecules which will induce fluorescence quenching for the rare earth complex by collision quenching or vibration relaxation. So, an effective way to get high PL of Tb^{3+} is to keep the TAP in an isolated environment with sufficient volume which the calcined MCM-41(MA) provides.

Figure 5 exhibits the excitation spectra of TAP, TAPMA, and TAPMB under emission at 544 nm. TAPMA-b (prepared by physical mixing of MA and TP powders

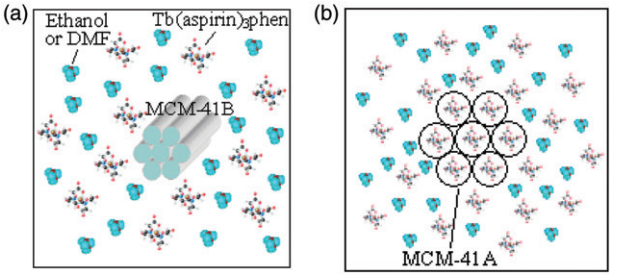

Figure 4. Schematic views of the two assembly systems in figure 3 (b) and (c) correspondingly. (a) TAPMB system in which most of the TAP molecules are distributed in the mixture of ethanol and DMF solution; (b) TAPMA system in which most of the TAP molecules are separated from solvent molecules, and are incorporated into the channels of MA.

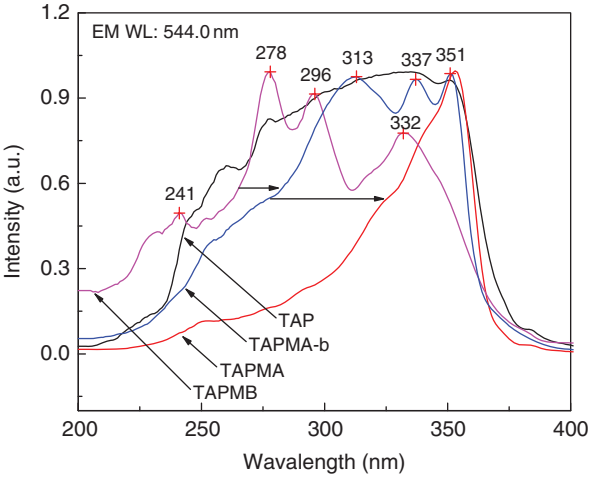

Figure 5. Excitation spectra of the solid powder of TAPMA-b, TAPMA, TAPMB, and TAP under emission at 544 nm at room temperature (300 K); the emission slit is 2.5 nm. All excitation data have been normalized.

by grinding for 30 min) was also prepared for a comparison, giving the information on the relationships between the organic host and the inorganic guest. Another excitation spectrum of aspirin (figure 6) must be given before our discussion on the PL mechanism. The excitation peak curve of aspirin attributed to $n \rightarrow \pi^*$ transition of carbonyl group, and $\pi \rightarrow \pi^*$ transition of benzene ring separately, is similar to the left part of the TAP curve, from 240 to 314 nm. Therefore, we also gain indirect but important information. The widest peak is in the range $340 \sim 375$ nm in the excitation spectrum of TAP, in which the strongest peaks that appear around 335 and 351 nm come from other transitions. Two possible transitions can be assigned as source of the two peaks, the first is the $^7F_6 \rightarrow {}^5D_1$ and $^7F_6 \rightarrow {}^5D_2$ transition from Tb^{3+}, and second is the absorption of phenanthroline. In order to ascertain the original sources of these peaks, EAPMA (Eu(aspirin)$_3$phen-MCM-41A) was synthesized. Two similar peaks at the same wavelength, 335 and 351 nm, were observed in the excitation spectrum of EAPMA (figure 7), which negates the first hypothesis directly. It is impossible for the transition between the silica wall and the Tb^{3+}, for that wall only has a very weak

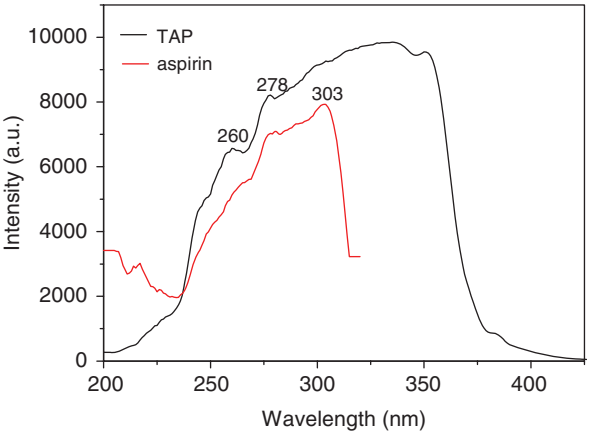

Figure 6. Excitation spectra of the solid powder of TAP and aspirin under emission at 544 nm at room temperature (300 K); the emission slit is 2.5 nm.

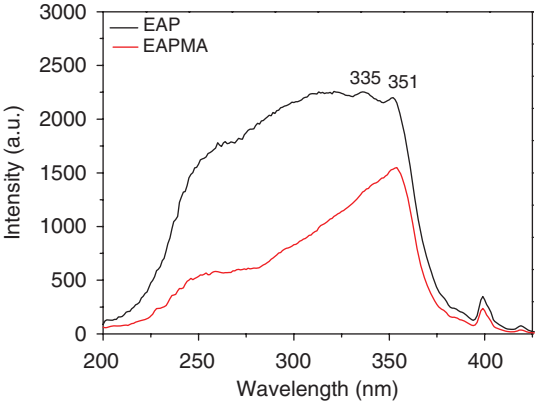

Figure 7. Excitation spectra of the solid powder of EAP (Eu(aspirin)$_3$phen) and EAPMA (Eu(aspirin)$_3$phen-MCM-41A) under emission at 544 nm at room temperature (300 K); the emission slit is 2.5 nm.

absorption in the range of 200 ~ 400 nm (figure 8). It is hard to observe the excitation peaks of MCM-41 in any of the TAPMA, TAPMB, or TAPMB-b system.

The excitation spectra of TAPMB and TAPMA-b, where TAP is absorbed on external surfaces, appear band split compared with that of TP, and only a narrow peak at 351 nm is left in the excitation spectrum of TAPMA, implying that the TAP exists in different surface environment. In addition, the main excitation peaks, from 278 to 353 nm, of the three systems vary regularly, shifting to lower energy (longer wavelength) from high, presented in table 3. These results imply that the different surface will weaken the excitation band of aspirin, and the energy for the PL of Tb^{3+} in the pores of MCM-41 is only from the energy absorption of phen.

Figure 9 shows that the intensity of the emission band around 415 nm in TAPMB, TAPMA-b, and TAPMA systems decreases regularly relative to the intensity of $^5D_4 \rightarrow {}^7F_5$ transition of Tb^{3+}. We consider the 410 nm band to be related to one of the transitions of aspirin which are detected in its emission spectrum (figure 10).

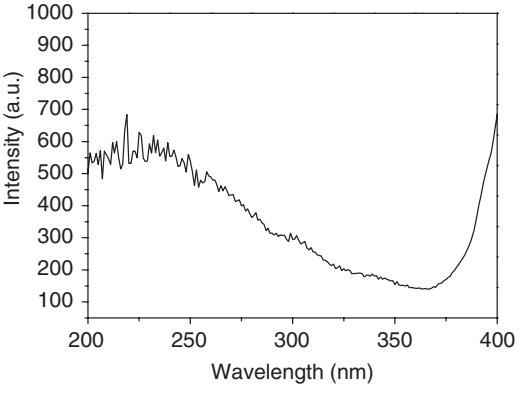

Figure 8. Excitation spectra of MA powder under emission at 544 nm at room temperature (300 K); the emission slit is 2.5 nm.

Table 3. Excitation, emission bands and I_L/I_{Ln} ratio I, where I_L and I_{Ln} are the relative emission intensity values of 400 and 544 nm under excitation at 335 nm, respectively, of the four solid systems.

Number	Product	Excitation band (nm)	Emission band (nm)	I (a.u.)
1	TAPMB	278, 296, 332	404, 489, 543, 583, 620	2.685
2	TAPMA-b	313, 337, 351	412, 491, 544, 583, 620	0.274
3	TAPMA	353	416, 490, 542, 583, 620	8.860×10^{-3}
4	TAP	233 ~ 380	373, 490, 541, 583, 621	1.609×10^{-3}

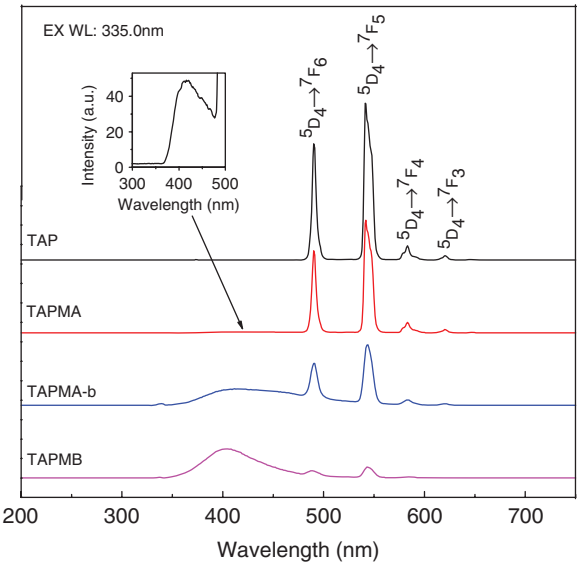

Figure 9. Emission variation of four solid systems, TAP, TAPMA, TAPMA-b, and TAPMB, under excitation at 335 nm at room temperature (300 K); the excitation slit is 2.5 nm.

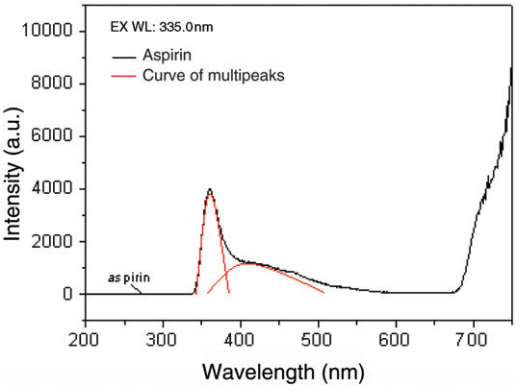

Figure 10. Emission spectrum of aspirin powder under excitation at 335 nm at room temperature (300 K); the excitation slit is 2.5 nm.

Two emission peaks were separated from the curve of multipeaks, one at 360 nm and the other at 415 nm.

Therefore, a parameter, $I_L/I_{Ln} = I$ (where I_L is the emission intensity of 400 nm band and the I_{Ln} is the emission intensity of 544 nm band) is introduced to the four solid systems, TAP, TAPMA, TAPMA-b, and TAPMB, to describe the special PL phenomenon. The values I presented in table 3 decrease from No.1 to No.3, in accord with shift of the excitation peaks from low wavelength to high; I of the free TAP is the smallest. We suggest that it has direct relationships with the different types of silica surface of MCM-41 [18, 19], that is the internal and the external surfaces of MA, and the external surface of MB.

The chemical environment of the silica surface, such as different types or content of silanol groups, influences the green PL of Tb^{3+}. The internal surface of MA is covered with siloxane bonds and single silanol groups, and external surface is covered with geminal silanol groups. Compared with TAP on the external surface of MCM-41A, the excitation peaks at 313 and 337 nm disappear for TAP on the internal surface of MCM-41A while the peaks of TAPMB appear at lower wavelength at 241, 287, 296, and 332 nm for which the high content of silanol groups (Si–OH) are responsible. Four characteristic emission peaks ascribed to the $^5D_4 \rightarrow {}^7F_6$, $^5D_4 \rightarrow {}^7F_5$, $^5D_4 \rightarrow {}^7F_4$, and $^5D_4 \rightarrow {}^7F_3$ transitions of Tb^{3+} are detected in each emission spectrum.

The excitation and emission of the rare earth complex is presented in figure 11. First, the ground states (S_0) of aspirin and phen are excited to the excited states (S_1) by absorbing energy, then parts of the energy are released by S_1–S_0 transition with ligand fluorescence. As the S_1 energy level of aspirin is higher than that of phen, the energy transfer also can take place between S_1 states of aspirin and phen by internal conversion. Second, intersystem crossing takes place inside phen, from which the triplet state T_1 of phen gains energy besides its absorption. It is necessary for the T_1 state of phen to have higher energy than the resonance energy level $^5D_4$ (Tb^{3+}) if a high fluorescence quantum efficiency of the rare earth ions is wanted, and the phosphorescence of phen is also suppressed. The last process is that the energy is transferred to $^5D_4$ (Tb^{3+}) from the T_1 state of phen by intramolecular energy transfer, and then the electron in the $^5D_4$ returns to the ground state ($^7F_{J,\,J=0,1,\sim,6}$) with a strong fluorescence emission.

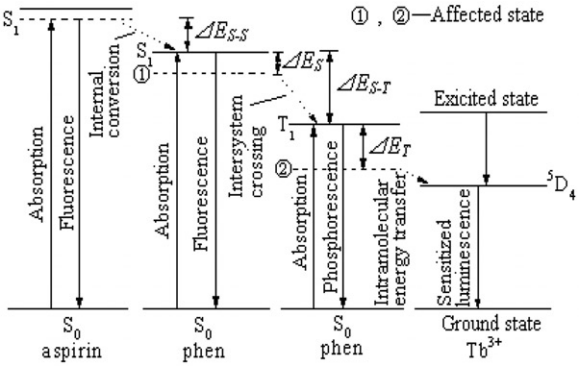

Figure 11. Energy transfer in the intersystem of TAP.

From figure 11, it can be seen that the S_1 and T_1 states of phen decrease by ΔE_S and ΔE_T, respectively, as the stabilization energy, and the value of ΔE_T is larger than ΔE_S in that the polarity of triplet state T_1 is higher than that of singlet S_1, leading to increase of the potential energy difference ΔE_{S-S} (the difference of S_1 state of aspirin and S_1 state of phen) and ΔE_{S-T} (the difference of S_1 state of phen and T_1 state of phen) correspondingly if one takes the S_1 state of aspirin as a static reference object. Otherwise, the difference ΔE_{T-Ln} of T_1 state of phen and $^5D_4$ (Tb^{3+}) also decreases by a certain degree.

When the lattice field, including the internal and external lattice fields on the silica wall surface, has strong negative effect on the absorption energy of ligands, the fluorescence quantum yield of Tb^{3+} depending on the energy transfer efficiency η, $\eta = \eta_{S-T}, \eta_{T-L}$, where η_{S-T} is the energy transfer efficiency of $S_1 - T_1$ of phen, and η_{T-L} is the energy transfer efficiency of T_1 (phen) – $^5D_4$ (Tb^{3+}), drops quickly as a result of the decrease in η_{S-T} and η_{T-L}. When ΔE_{S-T} becomes larger, the intersystem crossing probability inside the phen molecule and the η_{S-T} both decrease. Additionally, excessive reduction of ΔE_{T-Ln} can decline the η_{T-Ln} and the energy transfer rate constant K_{ET} according to Dexter's theory [20] of solid sensitization luminescence. Dexter's theory suggests that the energy transition from ligand to the center ion is ascribed to self-spin forbidden and depends on the energy difference and the energy matching between the triplet state energy level and the resonance energy level. The smaller the energy difference, the more favorable it is for the energy transfer to the rare earth ion from ligands. However, the small the energy transfer rate constant k_{ET} will also result in a greater energy loss and a decrease of fluorescence quantum yields of the rare earth ion. The intensity of aspirin's fluorescence around 400 nm attributed to energy transfer to S_0 from S_1 can be enhanced by increase of ΔE_{S-S} because the vibrational relaxation rate between the two S_1 states of aspirin and phen decreases. Based on figures 9 and 11, table 3, and the analyses above, we conclude that the effect of the external surface of MB on the ligands is more than that of the external surface of MA which is more than that of the internal surface of MA. In addition, the band splitting and shift in excitation spectra displayed in figure 5 can also be easily explained.

4. Conclusions

The system TAPMA was synthesized by self-assembly at room temperature. A new synthesis process, heat treating, was introduced for TAP, which is more suitable for MA. The results from XRD patterns show that TAPMA is a typical hexagonally ordered pore structure mesoporous material, and TAP can increase the lattice order of the silica surface. Compared with MA, the specific surface area of TAPMA decreases by 465.9905 $m^2 g^{-1}$, implying that most of TAP has been confined inside the channels of MA. The excitation and emission spectra indicate that the energy for PL of Tb^{3+} in the pores of MCM-41 is only from energy absorption of phen. Different chemical environment of the silica surface, such as the different types or contents of silanol groups, influence the green PL of Tb^{3+}. We suggest that the effect of external surface of MB on the ligands is more than that of the external surface of MA, which is more than that of the internal surface of MA. The PL photos and the emission spectrum show that the PL properties of TAP incorporated into the channels of MCM-41MA have not diminished. Work is in progress to extend potential applications of the rare earth complex and the mesoporous silica to optical devices, and to show the special effect of the chemical micro-environment in the mesoporous on the energy shifts in the rare earth complex.

References

[1] C.T. Kresge, M.E. Leonowicz, W.J. Roth, J.C. Vartuli, J.S. Beck. *Nature*, **359**, 710 (1992).
[2] J.S. Beck, J.C. Vartuli, W.J. Roth, M.E. Leonowicz, C.T. Kresge, K.D. Schmitt, C.W. Chu, D.H. Olson, E.W. Sheppard, S.B. McCullen, J.B. Higgins, J.L. Schlenker. *J. Am. Chem. Soc.*, **114**, 10834 (1992).
[3] P. Selvam, S.K. Bhatia, C.G. Sonwane. *Ind. Eng. Chem. Res.*, **40**, 3237 (2001).
[4] C.P. Wei, S.Z. Li, B. Zhou, C.J. Peng, K.J. Zhen. *Chem. Res. Chin. Univ.*, **22**, 371 (2006).
[5] T. Maschmeyer, F. Rey, G. Sankar, J.M. Thomas. *Nature*, **378**, 159 (1995).
[6] J.R. Gallo, H.O. Pastore, U Schuchardt. *J. Catal.*, **243**, 57 (2006).
[7] B. Munoz, A. Ramilla, P.J. Pariente, I. Diaz, R.M. Vallet. *Chem. Mater.*, **15**, 500 (2003).
[8] C.Y. Lai, B.G. Trewyn, D.M. Jeftinija, K. Jeftinija, S. Xu, S. Jeftinija, V.Y. Lin. *J. Am. Chem. Soc.*, **125**, 4451 (2003).
[9] Q. Xu, L. Li, R. Xu. *Chem. Mater.*, **14**, 549 (2002).
[10] L. Fu, Q. Xu, H. Zhang, L. Li, Q. Meng, R. Xu. *Mater. Sci.*, **88**, 68 (2002).
[11] A.N. Gleizes, A. Fernandes, G. Dexpert. *Electrochem. Soc. Interface*, **8**, 565 (2003).
[12] H.R. Li, J. Lin, H.J. Zhang, L.S. Fu. *Chem. Commun.*, 1212 (2001).
[13] Q.H. Xu, H.W. Li, L.S. Li, Y.C. Zou, R.R. Xu. *Chem. Res. Chin. Univ.*, **24**, 1758 (2003).
[14] D.L. Tao. *Spectrosc. Spect. Anal.*, **21**, 740 (2001).
[15] N. Duan, X.Q. Zhang, X. Gao, S. Liu, X.X.R. Xu. *Spectrosc. Spect. Anal.*, **21**, 267 (2001).
[16] J. Aguado, D.P. Serrano, J.M. Escola. *Microporous Mesoporous Mater.*, **34**, 43 (2000).
[17] K.S.W. Sing, D.H. Everett, R.A.W. Haul, L. Moscow, R. Apierotti, T. Rouquerol, T. Siemienew-ska. *Pure Appl. Chem.*, **57**, 603 (1985).
[18] X.S. Zhao, G.Q. Lu, A.K. Whittaker, G.J. Millar, H.Z. Zhu. *J. Phys. Chem. B*, **101**, 6525 (1997).
[19] Y. Inaki, H. Yoshida, T. Yoshida, T. Hattori. *J. Phys. Chem. B*, **106**, 9098 (2002).
[20] D.L. Dexter. *J. Chem. Phys.*, **21**, 836 (1995).